Coupled otolith and foraminifera oxygen and carbon stable isotopes evidence paleoceanographic changes and fish metabolic responses

Konstantina Agiadi[1], Iuliana Vasiliev[2], Geanina Butiseacă[3], George Kontakiotis[4], Danae Thivaiou[5], Evangelia Besiou[4], Stergios Zarkogiannis[6], Efterpi Koskeridou[4], Assimina Antonarakou[4], Andreas Mulch[2]

[1] Department of Geology, University of Vienna, Josef-Holaubek-Platz 2 (UZA II), 1090, Vienna, Austria
[2] Senckenberg Research Biodiversity and Climate Research Centre, Senckenberganlage 25, 60325, Frankfurt am Main, Germany
[3] Department OF Geosciences, Institute of Archaeological Sciences, Palaeoanthropology, Eberhard Karls Universität Tübingen, Rümelinstraße 23, 72070, Tübingen, Germany
[4] Department of Historical Geology and Palaeontology, Faculty of Geology and Geoenvironment, National and Kapodistrian University of Athens, Panepistimioupolis, 15784, Athens, Greece
[5] Department of Earth Sciences, University of Oxford, South Parks Road, Oxford, OX1 3AN, UK
[6] Natural History Museum of Basel, Augustinergasse 2, 4051 Basel, Switzerland

Correspondence to: Konstantina Agiadi (konstantina.agiadi@univie.ac.at)

Abstract. Capturing the mechanisms leading to the local extirpation of a species in deep-time is a challenge. Combining stable oxygen and carbon isotopic analyses on benthic and planktonic foraminifera and the otoliths of pelagic and benthic fish species, we reveal here the paleoceanographic regime shifts changes that took place in the Eastern Mediterranean from 7.2 to 6.5 Ma, in the precursor phase to the Messinian Salinity Crisis, and discuss the fishes' response to these events. The step-wise restriction of the Mediterranean–Atlantic gateway impacted the Mediterranean fishes' metabolisms, particularly those dwelling in the sea bottom. An important shift in the Mediterranean paleoceanographic conditions took place between 6.951 and 6.882 Ma, from predominantly temperature to salinity control, which was probably related to stratification of the water column. A regime shift at 6.814 Ma due to change in the influx amount, source and/or preservation of organic matter led a pelagic–benthic decoupling of the fish fauna. The oxygen isotopic composition of the benthic fish otoliths expresses higher salinity of the lower part of the water column at that time, and is accompanied by a rapid increase and then drop in the carbon isotopic compositions of the otoliths (which is metabolic rate proxy) of the benthic fish, ultimately leading to the local extirpation of the species. Overall, our results confirm that otolith stable oxygen and carbon isotopes are promising proxies for paleoceanographic studies and, when combined with those of foraminifera, can reveal changes in the life history and migration patterns of teleost fishes in deep time.

This manuscript has been submitted for discussion to the journal Biogeosciences.

1 Introduction

The paleoceanographic changes in the Mediterranean during the Messinian (7.25–5.33 Ma) and their impact on higher organisms can offer unique insights into the resilience of marine ecosystems under extreme environmental changes. Late Miocene climate cooling (Herbert et al., 2016) superimposed on the gradual restriction of the marine gateway with the Atlantic starting at the Tortonian/Messinian boundary (Krijgsman et al., 1999; Flecker et al., 2015) led to profound environmental changes in the Mediterranean, culminating in the Messinian Salinity Crisis (MSC; 5.97–5.33 Ma; Hsü et al., 1973). The basin's restriction resulted in high-amplitude shifts in sea surface temperature (SST) and salinity (SSS), and episodic water-column stratification and dysoxia on the sea bottom, even before the MSC (e.g., Moissette et al., 2018; Vasiliev et al., 2019; Sabino et al., 2020; Bulian et al., 2021; Kontakiotis et al., 2022; Mancini et al., 2024). However, the impact of these events on higher organisms such as fishes remains unclear. In the Early Messinian, the presence of new endemics (Girone et al., 2010) and Paratethyan-affinity fish species (Schwarzhans et al., 2020) in the Mediterranean has been attributed to the changing paleoceanographic conditions. This study presents a new approach on how climate affected marine life in the geological past, based on oxygen and carbon isotopic analyses of otoliths, aiming to test the hypothesis that the pre-MSC amplitude of changes in important paleoceanographic parameters (SST, SSS, organic matter source and primary productivity) had a negative impact on the physiology of marine fishes, and to distinguish the principal parameter controlling the fish populations.

Otoliths are accretionary, mostly aragonitic structures in the inner ear of teleost fishes, and they are metabolically inert, making them excellent paleoceanographic archives (Campana, 1999). The oxygen isotope ratio in otoliths ($\delta^{18}O_{oto}$) is a function of temperature and the oxygen isotopic composition of ambient water, which also depends on salinity: $\delta^{18}O_{oto}$ is not affected by somatic growth or the otolith precipitation rate, but species-specific lifestyle patterns can confound the signal (Kalish, 1991). The carbon isotopic composition of fish otoliths ($\delta^{13}C_{oto}$) registers the isotopic signatures of the fish's diet and the dissolved inorganic carbon (DIC) in ambient water (Kalish, 1991; Solomon et al., 2006; Trueman et al., 2016; Chung et al., 2019a). $\delta^{13}C_{oto}$ is a proxy of fish metabolic rate (Wurster and Patterson, 2003; Solomon et al., 2006; Trueman et al., 2016; Chung et al., 2019a, b; Martino et al., 2020; Smoliński et al., 2021; Trueman et al., 2023; Jones et al., 2023), reflecting the amount of energy the fish uses to live and grow, which impacts its behavior and resilience in the face of environmental change (Gauldie, 1996; Chung et al., 2019a). At the evolutionary level, higher metabolic rates in a population are generally expected to lead to higher genetic mutation rates (Trueman et al., 2016). In addition, $\delta^{13}C_{oto}$ is linked to oxygen consumption through the metabolic oxidation of dietary carbon (Chung et al., 2019b), while high metabolic rate results in higher oxygen consumption, higher activity, higher respiration and greater carbon export (Chung et al., 2019a). As a result, respiratory (or metabolic) carbon has a 15‰ lower $\delta^{13}C$ than DIC (Kroopnick, 1985).

In this study, in order to investigate the link between fish physiology and paleoceanographic change due to the restriction of the marine gateways connecting the Mediterranean Sea with the Atlantic Ocean in the Late Miocene, we first detect the regime shifts by analyzing time-series of independently obtained proxies. Then, we examine the fishes' responses by

comparing $\delta^{18}O_{oto}$ and $\delta^{13}C_{oto}$ time-series obtained for two very common zooplanktivorous species, the pelagic *Bregmaceros albyi* and the benthic *Lesueurigobius friesii*, from the Eastern Mediterranean for the interval 7.2–6.5 Ma.

2 Material and Methods

2.1 Material and sampling

Forty-seven sediment samples were collected from the ~25-m–thick pre-MSC Messinian laminated (sapropelic) and homogeneous marls succession of Agios Myron (Fig. 1; N 35°23'35.90", E 25°12'67.91", Crete Island, Eastern Mediterranean). A detailed description of the Agios Myron section is provided elsewhere (Zachariasse et al., 2021; Kontakiotis et al., 2022; Butiseacă et al., 2022).

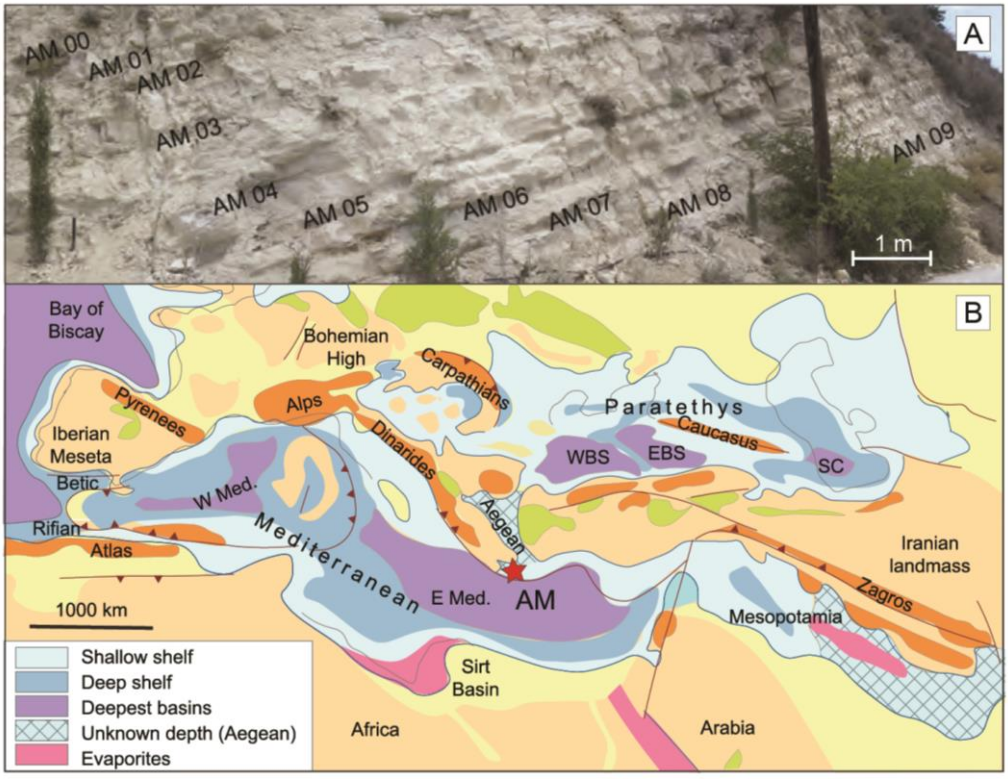

Figure 1: Study section. A) Photograph of the section showing the lithological alternations and sampling approach. B) Paleogeography map for the Mediterranean-Paratethys domain during late Miocene (Ilyina et al., 2004). Note the paleolatitudinal location and their approximate position within the late Miocene Mediterranean basin for Agios Myron (AM).

The samples were wet-sieved using various mesh sizes (minimum 63 μm). Up to five individuals each of the shallow-dwelling planktonic foraminifer species *Globigerinoides obliquus* and the benthic foraminifer *Cibicides (pseudo)ungerianus* were picked from the 250–300 μm sieve fraction of the same samples, according to standard practices (Seidenkrantz et al., 2000; Elderfield et al., 2002). The otoliths were handpicked from the sieved sediment residues and identified to species

level. From the picked specimens, the two target species, *Bregmaceros albyi* and *Lesueurigobius friesii*, were identified in 20 and 14 samples, respectively. Single otoliths from each level (and duplicates from samples AM05 and AM20C) were measured (L: length and W: width), cleaned and analyzed. We selected well-preserved otoliths, making sure that all their morphological characteristics were still present and that there were no particular coloration and/or signs of bioerosion or encrustation that may point toward extensive diagenetic alteration (Agiadi et al., 2022). The two fish species, whose otoliths were analyzed, were selected because of: a) their great abundance and frequency in Neogene and Quaternary Mediterranean marine sediments, which would render their isotopes useful as paleoceanographic proxies, and b) their well-established ecology, allowing more accurate interpretation of isotopic analyses results. Only the otoliths of adult individuals were analyzed to avoid differences in species-specific vital effects that affect isotopic ratios (Darnaude et al., 2014).

2.2 Oxygen and carbon isotopic analyses on otoliths and planktonic foraminifera

The otoliths and the foraminifera specimens were sonicated in methanol for about 10 s to remove clay particles adhering to the tests and rinsed at least five times in ultraclean water. Randomly selected specimens of foraminifera and otoliths were observed using a Jeol JSM 6360 scanning electron microscope or a stereoscope, respectively, to confirm their good preservation state (Antonarakou et al., 2019; Agiadi et al., 2022). Stable carbon and oxygen isotopic analyses were performed using a Thermo Scientific MAT 253 Plus mass spectrometer coupled to a GasBench II with carbonate option, in continuous flow mode, using a thermostated sample tray and a GC PAL autosampler at the Goethe Universität – Senckenberg BiK-F Joint Stable Isotope Facility in Frankfurt am Main, Germany. Analytical precision was 0.08‰ for $\delta^{18}O$ and 0.06‰ for $\delta^{13}C$. In both cases, we analyzed replicates of 10% of the data reveal to confirm reproducibility of the results; natural sample variability was better than 0.1‰. Results are reported against the Vienna Pee Dee Belemnite (VPDB) standard using the δ notation and expressed in per mil (‰).

2.3 Other biogeochemical data used for interpretation

The results of the otoliths isotopic analyses were additionally interpreted considering: a) the $\delta^{18}O$ and $\delta^{13}C$ of *C. (pseudo)ungerianus* (Zachariasse et al., 2021); b) paleodepth estimates based on foraminifera (Zachariasse et al., 2021); c) Tetra Ether Index (TEX^{H}_{86})-derived SST and $TEX_{86}{}^{H}$-$\delta^{18}O_{G.obliquus}$-based SSS estimates (Kontakiotis et al., 2022); d) the ratio of isoprenoidal glycerol dialkyl glycerol tetraethers 2 and 3 (isoGDGT2/isoGDGT3) (Kontakiotis et al., 2022), which increases with isoGDGTs input from subsurface-dwelling archaea (Schouten et al., 2002); and e) BIT (branched and isoprenoid tetraether) index values which reflect the source of organic matter (Butiseacă et al., 2022).

2.4 Ecological information about the selected fish species

Bregmaceros albyi (Sauvage, 1880) is one of the most common extinct fish species in the Neogene and Quaternary Mediterranean, found both as articulated skeletons and otoliths in great abundances (Landini and Sorbini, 2005; Agiadi and Karakitsios, 2012; Agiadi et al., 2013). *Bregmaceros* spp. are small pelagic fishes with 14 extant species distributed in the

Atlantic, Indian and Pacific Oceans and mostly occupying the euphotic zone (FishBase, 2024). Even though *Bregmaceros* sp. was still present in the Eastern Mediterranean until the Late Pleistocene (Cornée et al., 2019), *B. nectabanus* Whitley, 1941 is the only representative currently inhabiting the basin, and it is considered a non-indigenous species (Agiadi and Albano, 2020). *Bregmaceros nectabanus* has reported up to 350 m depth, but is also able to migrate temporarily into anoxic waters (FishBase, 2024). *Bregmaceros* spp. feed on zooplanktonic invertebrates, particularly copepods, and some species also on phytoplankton (FishBase, 2024).

Lesueurigobius friesii (Malm, 1874) is a benthic, subtropical marine fish living at depths between 10–130 m in the East Atlantic and the Mediterranean and feeding mainly on polychaetes, small crustaceans and mollusks (FishBase, 2024). It has a preferred temperature today between 7.2 and 18.4 °C, with a mean of 10.4 °C (AquaMaps: predicted range maps for aquatic species). Its presence in the Mediterranean fossil record goes back to the late Tortonian (Agiadi et al., 2017) and it is common in shallow-waters until the present (Agiadi et al., 2019; Agiadi and Albano, 2020). As a benthic species, *L. friesii* is site-attached, and therefore its isotopic composition is expected to closely reflect the local conditions on the sea floor (Mirasole et al., 2017).

2.5 Statistical analyses

In order to test for the response of the fishes to significant changes in the paleoceanographic parameters, we used the Sequential T-test Analysis of Regime-Shifts (STARS) algorithm (Rodionov, 2004) to identify regime shifts based on the organic biomarker and foraminifera isotopic data. Regime shifts are abrupt changes between two natural states of climate or of an ecosystem, where each state can have its own internal variability (Kerr, 1992; Scheffer, 2020). The STARS algorithm allows detecting regime shifts robustly even at the ends of a time series (Rodionov, 2004). Because the STARS algorithm can only be applied to variables that have a normal distribution, we first tested for normality using the Shapiro-Wilk test. For those variable that did not have a normal distribution (here, $\delta^{13}C_{B.albyi}$, $\delta^{18}O_{L.friesii}$, BIT, and $\delta^{13}C_{C.ung}$), we used instead the L-method (Lanzante, 1996), which is based on the Mann-Whitney U test. In STARS, we set the *p*-value at 0.05, Huber's weight parameter of 1, and the window size at 10. The selection of window size is generally arbitrary and can strongly affect the sensitivity of the algorithm. For this reason, we confirmed that the identified regime shifts were also detected when using window size values from 5 to 20.

We investigated the existence of size-dependent patterns in the carbon and oxygen isotopic composition of the otoliths of the two species by testing for statistical correlation between the otolith size and the $\delta^{18}O_{oto}$ and $\delta^{13}C_{oto}$ values, since otolith size is linked to fish size through species-specific functions (Edelist, 2014). For these tests, we used the Spearman rank correlation coefficient (95% confidence level).

Furthermore, we tested for correlation between the $\delta^{18}O$ and $\delta^{13}C$ values of otoliths and foraminifera, and between these values and the SST and SSS values estimated by Kontakiotis et al. (2022) and the BIT index (Butiseacă et al., 2022), across the entire study interval of the Agios Myron section and considering lithological cyclicity (i.e. for sapropel levels because only data for six homogeneous marl levels were available). For these tests, we used the Spearman rank correlation

coefficient (95% confidence level). Based on the results of the regime shifts detection, we tested for correlation between these variables across the identified regimes.

The above analyses were performed in R (version 4.3.1) (R Development Core Team, 2023), and we used the packages *dplyr* (Wickham et al., 2023) and *rshift* (Room et al., 2020).

3 Results

3.1 Isotopic analysis results and size correlations

The $\delta^{18}O_{B.albyi}$ values range from −0.28 to 0.41‰ in the homogeneous marls, from −1.47 to 2.64‰ in the laminated marls, and from −0.63 to 0.05‰ in the silty marls in the lower part of the section. The $\delta^{18}O_{G.obliquus}$ values range from –0.84 to 0.44‰ in the homogeneous marls, from –1.36 to 0.79‰ in the laminated marls, and from –0.74 to 0.23‰ in the silty marls. The $\delta^{18}O_{L.friesii}$ values range from 2.14 to 4.3‰ in the homogeneous marls, from 2.32 to 4.11‰ in the laminated marls, and from 2.07 to 2.2‰ in the silty marls (Agiadi et al. 2024).

The $\delta^{13}C_{L.friesii}$ values range from −5.8 to −4.2‰ in the homogeneous marls, from −5.81 to −4.19‰ in the laminated marls, and from −5.41 to −4.68‰ in the silty marls in the lower part of the section. The $\delta^{13}C_{G.obliquus}$ values range from –0.18 to 0.46‰ in the homogeneous marls, from –0.35 to 1.49‰ in the laminated marls, and from 0.29 to 1.13‰ in the silty marls. The $\delta^{13}C_{B.albyi}$ values range from −5.92 to −5.23‰ in the homogeneous marls, from −9.02 to −3.71‰ in the laminated marls, and from −5.44 to −5.19‰ in the silty marls (Agiadi et al. 2024). There were no *Lesueurigobius friesii* otoliths in the samples younger than 6.653 Ma.

No correlation was detected between the isotopic values and otolith length at the 95% confidence level, with Spearman's rho values of 0.13 (p = 0.58) for $\delta^{13}C_{B.albyi}$, 0.11 (p = 0.70) for $\delta^{13}C_{L.friesii}$, −0.04 (p = 0.88) for $\delta^{18}O_{B.albyi}$ and −0.17 (p = 0.56) for $\delta^{18}O_{L.friesii}$.

For the Agios Myron record as a whole, there is a strong correlation between $\delta^{18}O_{G.obliquus}$ and SSS (rho = 0.78, p = 1.078e-05), but no correlation between $\delta^{18}O_{B.albyi}$ and SSS (rho = 0.12, p = 0.61) or $\delta^{18}O_{C.ung}$ and SSS (rho = 0.30, p = 0.17). However, we found moderate correlation between $\delta^{18}O_{B.albyi}$ and $\delta^{18}O_{L.friesii}$ (rho = 0.69, p = 0.04).

Examining the laminated marls only, we found moderate correlation between $\delta^{18}O_{B.albyi}$ and $\delta^{18}O_{G.obliquus}$ (rho = 0.55, p = 0.05), and $\delta^{18}O_{G.obliquus}$ and SST (rho = 0.60, p = 0.03). Strong correlation was found for the sapropel levels between $\delta^{18}O_{L.friesii}$ and $\delta^{18}O_{C.ung}$ (rho = 1, p = 0.02) and $\delta^{18}O_{G.obliquus}$ and SSS (rho = 0.93, p < 2.2e–16). No correlation was found between $\delta^{13}C_{B.albyi}$ and $\delta^{13}C_{G.obliquus}$ (rho = 0.06, p = 0.84), $\delta^{13}C_{L.friesiii}$ and $\delta^{13}C_{C.ung}$ (rho = –0.1, p = 0.95), $\delta^{18}O_{B.albyi}$ and SST (rho = –0.09, p = 0.77), $\delta^{18}O_{C.ung}$ and SST (rho = 0.24, p = 0.41), $\delta^{18}O_{B.albyi}$ and SSS (rho = 0.39, p = 0.17), or $\delta^{18}O_{C.ung}$ and SSS (rho = 0.24, p = 0.41). Combining the laminated marls with the silty marl levels in the analysis, we found moderate correlations between $\delta^{18}O_{B.albyi}$ and $\delta^{18}O_{G.obliquus}$ (rho = 0.50, p = 0.05), and $\delta^{18}O_{L.friesii}$ and $\delta^{18}O_{C.ung}$ (rho = 0.78, p = 0.05).

3.2 Regime shifts and responses

The Regime Shift Index (RSI) has positive values, which indicate the presence of regime shifts (95% confidence level), at: 1) 6.951 Ma for $\delta^{18}O_{G.obliquus}$ (*RS1*; RSI = 0.23), 2) 6.882 Ma for SST (*RS2*; RSI = 0.70), 3) 6.847 Ma for SSS (*RS3*; RSI = 0.85), and 4) 6.814 Ma for $\delta^{13}C_{G.obliquus}$ (*RS4*; RSI = 0.33). There is no correlation between any of the biogeochemical proxies used here from 7.166 to 6.951 Ma (*RS1*). After 6.951 Ma (*RS1*), very strong correlation was indeed found between $\delta^{18}O_{G.obliquus}$ and SSS (rho = 0.85, p < 2.39e–05). Examining the laminated marls, there is only a weak correlation between $\delta^{18}O_{B.albyi}$ and $\delta^{18}O_{G.obliquus}$ (rho = 0.56, p = 0.06) after 6.951 Ma, and the very strong correlation between $\delta^{18}O_{G.obliquus}$ and SSS (rho = 0.88, p < 9.166e–05). From 7.166 to 6.882 Ma (*RS2*), a moderate correlation was found between $\delta^{18}O_{G.obliquus}$ and SST (rho = –0.63, p = 0.04) but only a weak correlation between $\delta^{18}O_{G.obliquus}$ and SSS (rho = 0.58, p = 0.07). After 6.882 Ma (*RS2*), there is only very strong correlation between $\delta^{18}O_{G.obliquus}$ and SSS (rho = 0.93, p < 2.2e–16). From 7.166 until 6.847 Ma (*RS3*), $\delta^{18}O_{G.obliquus}$ is strongly correlated with SST (rho = –0.62, p = 0.03) but weakly correlated with SSS (rho = 0.54, p = 0.07), whereas after 6.847 Ma there is only very strong correlation between $\delta^{18}O_{G.obliquus}$ and SSS (rho = 0.94, p < 2.2e–16). From 7.166 until 6.814 Ma (*RS4*), a moderate correlation is found between $\delta^{18}O_{G.obliquus}$ and SSS (rho = 0.69, p = 0.006). After 6.814 Ma (*RS4*), the correlation between $\delta^{18}O_{G.obliquus}$ and SSS (rho = 0.94, p < 2.2e–16) becomes very strong.

4 Discussion

4.1 Paleoceanographic conditions

Our results evidence a significant correlation between otolith and foraminifera $\delta^{18}O$ at surface and at bottom waters, collected from the laminated and the silty marls at the base of the section. This result confirms $\delta^{18}O_{oto}$ as a promising proxy for paleoceanographic studies (as anticipated by e.g. Radtke et al., 1996; Thorrold et al., 1997; Darnaude et al., 2014), supporting the combined use of $\delta^{18}O$ measured on both otoliths and foraminifera to reveal changes in the life history and migration patterns of teleost fishes in deep time.

As expected, the $\delta^{18}O$ of the bottom-dwellers ($\delta^{18}O_{L.friesii}$ and $\delta^{18}O_{C.ung}$) have more positive values than those of the surface-dwellers ($\delta^{18}O_{B.albyi}$ and $\delta^{18}O_{G.obliquus}$), the benthic fish and foraminifera occupy the bottom of the water column, which is colder and more saline than the surface water (Fig. 2).

Sea surface salinity fluctuations in the eastern Mediterranean were the dominant controlling factor of the response of zooplankton and fishes already from 6.882 Ma (*RS2*) and until 6.5 Ma, as seen by the $\delta^{18}O_{G.obliquus}$–SSS and $\delta^{18}O_{B.albyi}$–SSS correlations. Between 7.166 Ma and 6.951 (*RS1*), surface conditions at Agios Myron were mostly controlled by SST, as shown by the correlation between $\delta^{18}O_{G.obliquus}$ and SST. For the interval between 6.951 (*RS1*) and 6.882 Ma (*RS2*), both SSS and SST drive the zooplankton and fish responses.

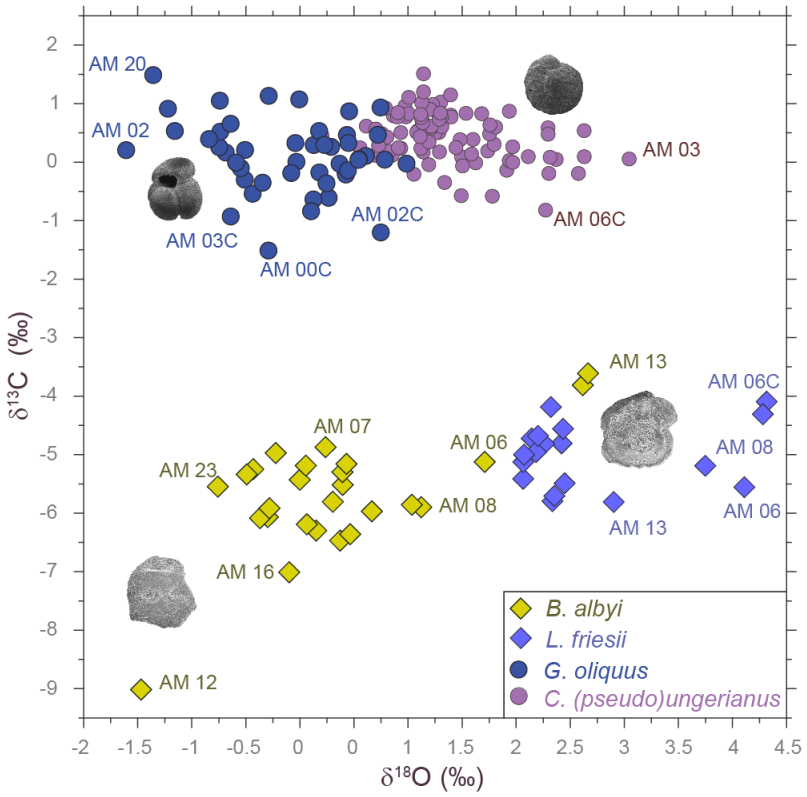

Figure 2: $\delta^{18}O$–$\delta^{13}C$ plot of the fish otolith and foraminifer samples analyzed from Agios Myron section. The four species clusters are clearly distinguished in the plot.

The regime shift of $\delta^{13}C_{G.obliquus}$ at 6.814 Ma (*RS4*; Fig. 3) takes place right after the positive $\delta^{18}O_{B.albyi}$ shift at 6.824 Ma, followed by a negative one at 6.806 Ma, mimicking the change in the Archaea community (isoGDGT2/isoGDGT3 index). Considering that $\delta^{18}O_{L.friesii}$ does not show a similar positive shift, we interpret the $\delta^{18}O_{B.albyi}$ pattern to reflect a short-lived event of remarkable negative water budget at 6.824 Ma (shown by Butiseacă et al., 2022). Subsequently, from 6.814 Ma until 6.5 Ma, $\delta^{18}O_{L.friesii}$ and $\delta^{18}O_{C.ung}$ exhibit increasing trends, in contrast to $\delta^{18}O_{B.albyi}$ and $\delta^{18}O_{G.obliquus}$, which suggests that the event at 6.824 Ma triggered persistent stratification and increased bottom-water salinity. This interpretation is also corroborated by the increase in abundance of Neogloboquadrinids (Zachariasse et al., 2021) that are indicators of high nutrient availability in a colder, stratified water column (Sierro et al., 2003), as well as with the presence of high-salinity–tolerant benthic foraminifera and the Mn/Al depletion at this time interval, suggesting decreased bottom-water oxygenation throughout the Mediterranean after a gateway restriction step at 6.8 Ma (Kouwenhoven et al., 2003; Sierro et al., 2003; Lyu et al., 2022). In contrast, the positive shift of $\delta^{18}O_{B.albyi}$ at 6.68 Ma is accompanied by an analogous shift of $\delta^{18}O_{L.friesii}$, reflecting similar changes in both surface and bottom waters, most likely due to temperature drop to 22 °C rather than salinity decrease that would drag the $\delta^{18}O_{oto}$ towards lower values (Kontakiotis et al., 2022).

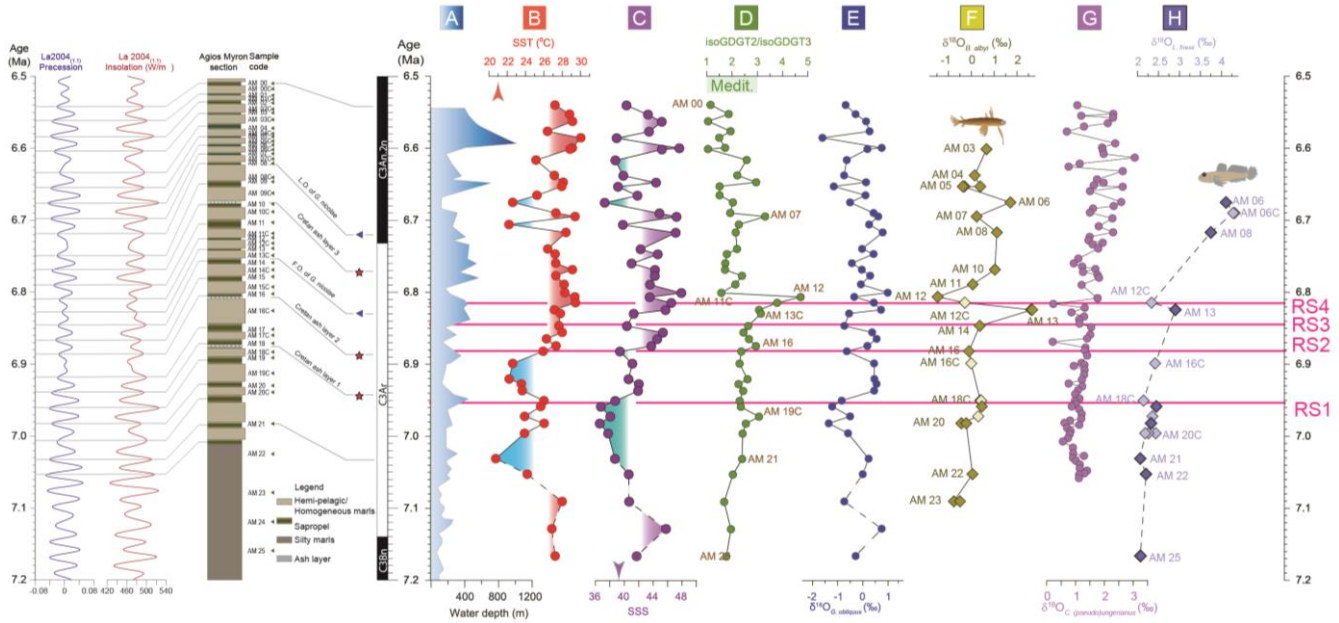

Figure 3: Agios Myron lithostratigraphic column, major bioevents and chronostratigraphy, in the precession and insolation framework for the time interval of the study (Laskar et al., 2004). A) paleobathymetric curve based on foraminifera (Zachariasse et al., 2021); B) sea surface temperature calculated based on TEX^{H}_{86}, C) sea surface salinities based on SST-TEX^{H}_{86} and $\delta^{18}O_{G.obliquus}$ (Kontakiotis et al., 2022); D) Ratio of isoprenoidal glycerol dialkyl glycerol tetraethers 2 and 3 (isoGDGT2/isoGDGT3) (Butiseacă et al., 2022); E) $\delta^{18}O$ of the shells of the planktonic foraminifer *Globigerinoides obliquus*; F) $\delta^{18}O$ of the otoliths of the pelagic fish *Bregmaceros albyi*; G) $\delta^{18}O$ of the shells of the benthic foraminifer *Cibicides (pseudo)ungerianus* (Zachariasse et al., 2021); and H) $\delta^{18}O$ of the otoliths of the benthic fish *Lesueurigobius friesii*. RS1–4 indicate the four regime shifts found in this study at 6.951 Ma for $\delta^{18}O_{G.obliquus}$, 6.882 Ma for SST, 6.847 Ma for SSS, and 6.814 Ma for $\delta^{13}C_{G.obliquus}$.

4.2 Fish metabolic response to paleoceanographic change

Carbon in otoliths comes from two sources: seawater and diet. Therefore, $\delta^{13}C_{oto}$ reflects changes in the seawater $\delta^{13}C$, which depends on pH, and in the fish's diet and metabolic rate. The carbon stable isotopic ratios of the fish otoliths here are more negative than those of the foraminifera (Fig. 2), which is expected since $\delta^{13}C_{diet}$ is more negative than $\delta^{13}C_{DIC}$. Considering $\delta^{13}C_{G.obliquus}$ and $\delta^{13}C_{C.ung}$ as reflecting $\delta^{13}C_{DIC}$ in surface and bottom waters, respectively (Mackensen and Schmiedl, 2019), we evaluate here the $\delta^{13}C_{oto}$ changes as indicative of changes in the metabolic responses of the two fish species.

For fish feeding on phytoplankton and zooplankton, such as the ones examined in this study, $\delta^{13}C_{oto}$ is negatively correlated with food availability and, therefore, with net primary productivity (Burton et al., 2011): under conditions of high (low) food availability, individual fishes with high (low) metabolic rates are more resilient and they would exhibit lower (higher) $\delta^{13}C_{oto}$ since they would be eating more, consequently acquiring less ^{13}C from their diet. In addition, $\delta^{13}C_{oto}$ may be positively or negatively correlated, or not correlated at all with temperature depending on the species, oceanographic conditions and

setting (Kalish, 1991; Martino et al., 2019). In the case of Agios Myron, no significant correlation is found between $\delta^{13}C_{B.albyi}$ (or $\delta^{18}O_{B.albyi}$ either), and SST or SSS. Both $\delta^{13}C_{B.albyi}$ and $\delta^{18}O_{B.albyi}$ show much wider ranges in the laminated than in the homogenous marls, but these are not accompanied by greater ranges of SST or SSS in the sapropelic levels (Kontakiotis et al., 2022). $\delta^{13}C_{B.albyi}$ alone could be explained by wider ranges in primary productivity and nutrient supply among the laminated marls. However, $\delta^{18}O_{B.albyi}$ adds complexity to this explanation, in that it requires the fishes also experience larger ranges of salinities/temperatures (compared to the homogeneous marl levels), which are not supported by SST and SSS. Alternatively, the $\delta^{13}C_{B.albyi}$ and $\delta^{18}O_{B.albyi}$ ranges (Figs. 3 and 4) could be attributed to shifts in the depth distribution of *B. albyi* to include deeper, even anoxic parts of the water column, as is common for the modern *B. nectabanus* (FishBase, 2024).

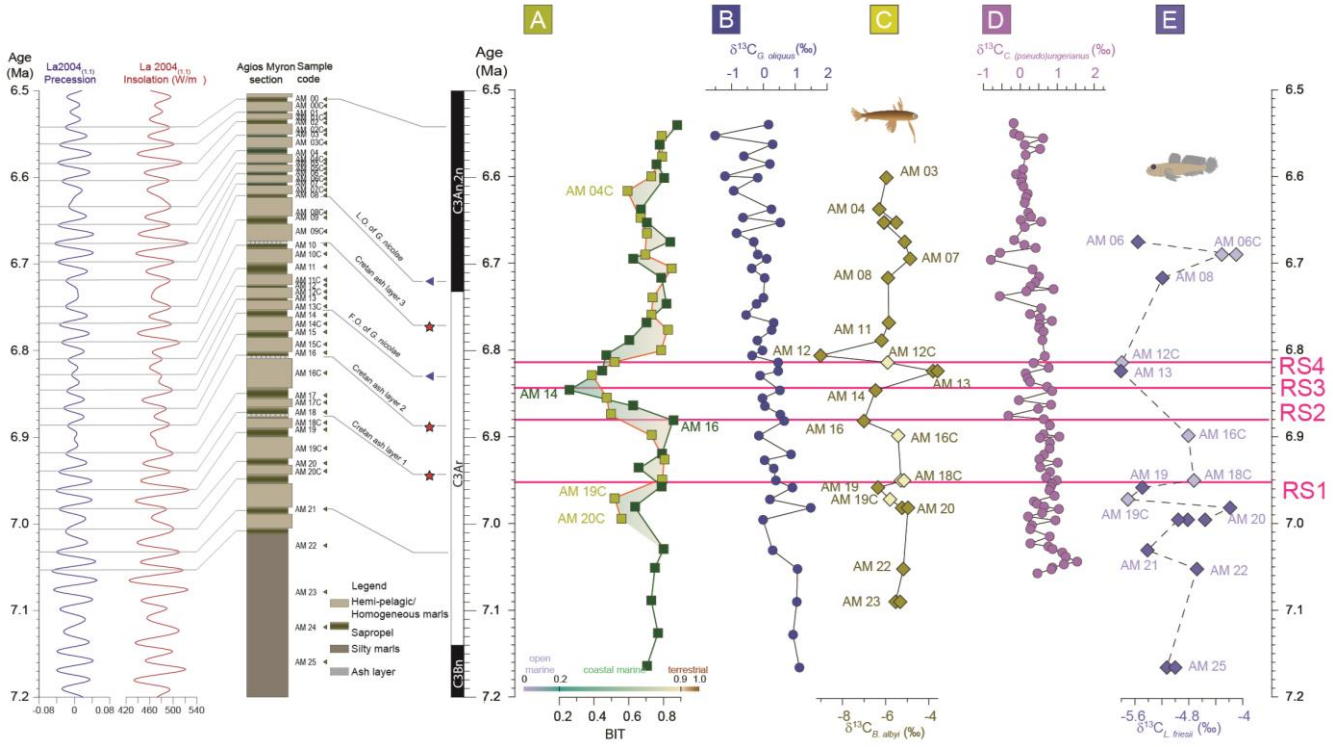

Figure 4: Agios Myron lithostratigraphic column, major bioevents and chronostratigraphy, in the precession and insolation framework for the time interval of the study (Laskar et al., 2004). A) Branched and Isoprenoid Tetraethers (BIT) index (Butiseacă et al., 2022); B) δ^{13}C of the shells of the planktonic foraminifer *Globigerinoides obliquus*; C) δ^{13}C of the otoliths of the pelagic fish *Bregmaceros albyi*; D) δ^{13}C of the shells of the benthic foraminifer *Cibicides (pseudo)ungerianus* (Zachariasse et al., 2021); E) δ^{13}C of the otoliths of the benthic fish *Lesueurigobius friesii*. RS1–4 indicate the four regime shifts found in this study at 6.951 Ma for $\delta^{18}O_{G.obliquus}$, 6.882 Ma for SST, 6.847 Ma for SSS, and 6.814 Ma for $\delta^{13}C_{G.obliquus}$.

Both surface and bottom-water DIC become depleted in ^{13}C from 7.2 to 6.5 Ma in the Agios Myron section (as both $\delta^{13}C_{G.obliquus}$ and $\delta^{13}C_{C.ung}$ show negative trends; Fig. 4). In the absence of a similar trend in the BIT index (i.e. a change in the source of organic matter), these trends reflect decreased productivity and ventilation of bottom waters, in line with the North

Atlantic and Western Mediterranean records (Hodell et al., 2001; van der Schee et al., 2016; Drury et al., 2018; Bulian et al., 2023, 2022). On the other hand, both $\delta^{13}C_{B.albyi}$ and $\delta^{13}C_{L.friesii}$ show negative peaks at 6.959, 6.824 and 6.806 Ma, which coincide with changes in the composition of the Achaea community (isoGDGT2/isoGDGT3; Fig. 3) and fall around the times of peaks in the BIT index. The statistical testing did not show a correlation between $\delta^{13}C_{B.albyi}$, $\delta^{13}C_{L.friesii}$, BIT and isoGDGT2/isoGDGT3, and the time interval of this study does not permit an investigation of any lagged responses. Therefore, we consider that these $\delta^{13}C_{B.albyi}$ and $\delta^{13}C_{L.friesii}$ negative peaks reflect events of crisis in the food availability (source and content) for surface and bottom-water fishes, which impacted the fishes' metabolism.

A single regime shift in $\delta^{13}C_{G.obliquus}$ is found at 6.814 Ma (*RS4*) and it coincides with a change in the Archaea community (isoGDGT2/isoGDGT3 index; Fig. 4; (Butiseacă et al., 2022). The event at 6.82–6.81 Ma has a strong impact on fish metabolism, as it is clearly seen first in the negative peak of $\delta^{13}C_{B.albyi}$ and then in the positive shifts of $\delta^{13}C_{B.albyi}$ and $\delta^{13}C_{L.friesii}$, which are accompanied by a BIT shift to increased relative contribution of terrestrial organic matter (Butiseacă et al., 2022) and to the maximum of isoGDGT2/isoGDGT3. Together with the positive $\delta^{18}O_{B.albyi}$ shift at 6.824 Ma that is attributed to a negative water-budget event (see section 4.1), we propose a temporary influx of high-nutrient terrestrial material at 6.814 Ma, leading to phytoplankton bloom and a consequent increase in zooplankton abundance, which provides more food for the fish population both in surface and bottom waters. After this point, $\delta^{13}C_{L.friesii}$ increases and peaks at 6.690 Ma (Fig. 4) indicating a corresponding decrease in metabolic rate, and then it abruptly drops at 6.675 Ma before the disappearance of *L. friesii* from Agios Myron and other Mediterranean sites (Karakitsios et al., 2017; Schwarzhans et al., 2020). At 6.690 Ma, there is a pronounced drop in $\delta^{13}C_{C.ung}$, but no corresponding change in $\delta^{13}C_{G.obliquus}$, $\delta^{18}O_{C.ung}$ or $\delta^{18}O_{G.obliquus}$, suggesting that deceased bottom-water ventilation, combined with basin deepening at the Agios Myron location (Zachariasse et al., 2021) resulted in the local extirpation of *L. friesii*.

5 Conclusions

In the pre-MSC Messinian, due to the restriction of the Mediterranean–Atlantic gateway, the Mediterranean experienced intense variability in temperature and salinity, but also changes in primary productivity and terrestrial influx, which resulted in increased stratification of the water column and decreased ventilation of the bottom waters (Fig. 5). Our results evidence turning points in the Mediterranean paleoceanographic conditions between 6.951 and 6.882 Ma, when salinity and its variation amplitude increase probably related to stratification of the water column, and at 6.814 Ma when there is a major disturbance in the influx amount and source of organic material to the basin driving a change in primary production. For fishes, the most important event is the regime shift at 6.814 Ma (*RS4*), after which we see a pelagic–benthic decoupling with $\delta^{18}O_{L.friesii}$ expressing the higher salinity of the lower part of the water column, as well as a rapid increase and then drop in the metabolic rate of the benthic fish ($\delta^{13}C_{L.friesii}$), ultimately leading to the local extirpation of the species.

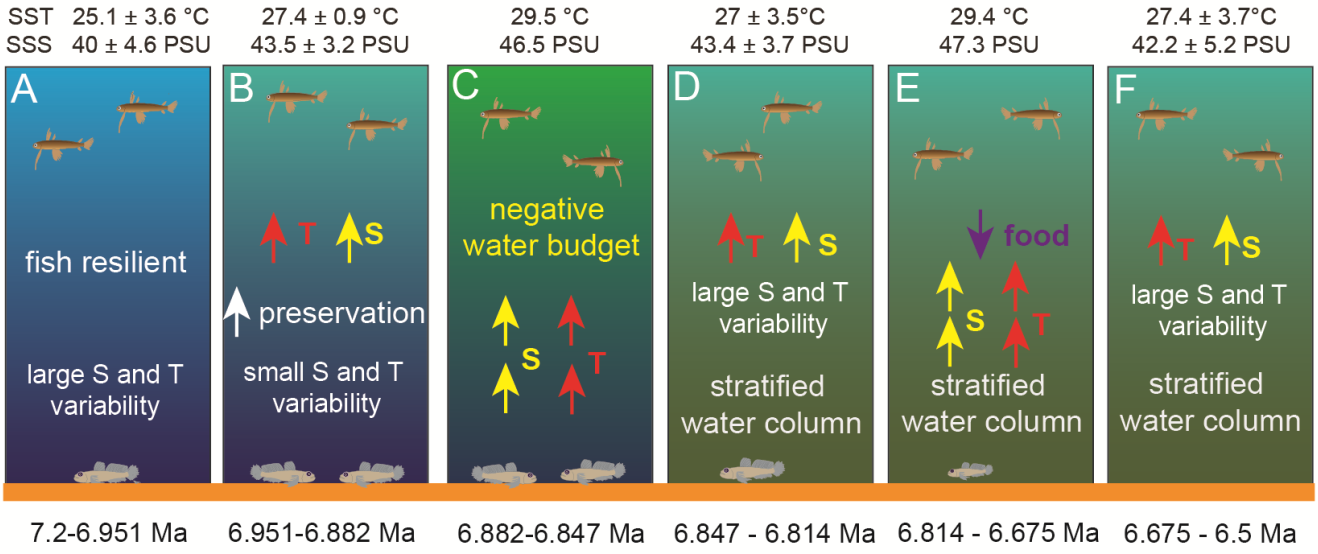

290 **Figure 5: Schematic model of the response of surface and bottom-dwelling marine fishes to the paleoceanographic and paleoclimatic changes taking place from 7.2 to 6.5 Ma in the Eastern Mediterranean.**

Data availability

Raw data for this manuscript are publicly available at: https://doi.org/10.5281/zenodo.10602427

Author contributions

295 Conceptualization: KA, IV; Data curation: IV, GK; Formal analysis: KA; Funding acquisition: KA, IV; Investigation: KA, IV, GB, GK, DT, EB, SZ, EK, AA, AM; Methodology: KA; Writing – original draft preparation: KA, IV; Writing – review & editing: GB, GK, DT, EB, SZ, EK, AA, AM.

Competing interests

The authors declare that they have no conflict of interest.

300 ## Acknowledgements

This work was supported by the Austrian Science Fund (FWF) project "Late Miocene Mediterranean Marine Ecosystem Crisis" (2022–2026), Grant DOI 10.55776/V986 (KA); by Greek national funds and the European Social Fund through the action "Postdoctoral Research Fellowships" of the Greek National Scholarships Foundation, project "Comparative study of

the Messinian Salinity Crisis effect on the Eastern Ionian and northern Aegean ichthyofauna" (2017–2019) (KA); and by the Greek-German collaboration project (IKYDA-DAAD): "Quantification of the environmental changes in the Eastern Mediterranean at the onset of the Messinian Salinity Crisis (Crete-Greece)" (QUANTMES) (IV). Collaboration for this project was facilitated by the COST Action CA15103 "Uncovering the Mediterranean salt giant" MEDSALT (2016–2020).

References

Agiadi, K. and Albano, P. G.: Holocene fish assemblages provide baseline data for the rapidly changing eastern Mediterranean, The Holocene, 30, 1438–1450, https://doi.org/10.1177/0959683620932969, 2020.

Agiadi, K. and Karakitsios, V.: Quaternary climatic variability modulates Bregmaceros Mediterranean distribution range, Proc. 10th Hell. Symp. Oceanogr. Fish. Athens, 1–6, 2012.

Agiadi, K., Koskeridou, E., Triantaphyllou, M., Girone, A., and Karakitsios, V.: Fish otoliths from the Pliocene Heraklion Basin (Crete Island, Eastern Mediterranean), Geobios, 46, 461–472, https://doi.org/10.1016/j.geobios.2013.07.004, 2013.

Agiadi, K., Antonarakou, A., Kontakiotis, G., Kafousia, N., Moissette, P., Cornée, J.-J., Manoutsoglou, E., and Karakitsios, V.: Connectivity controls on the late Miocene eastern Mediterranean fish fauna, Int. J. Earth Sci., 106, 1147–1159, https://doi.org/10.1007/s00531-016-1355-7, 2017.

Agiadi, K., Vasileiou, G., Koskeridou, E., Moissette, P., and Cornee, J.-J.: Coastal fish otoliths from the early Pleistocene of Rhodes (eastern Mediterranean), Geobios, 55, 1–15, https://doi.org/10.1016/j.geobios.2019.06.006, 2019.

Agiadi, K., Azzarone, M., Hua, Q., Kaufman, D. S., Thivaiou, D., and Albano, P. G.: The taphonomic clock in fish otoliths, Paleobiology, 48, 154–170, https://doi.org/10.1017/pab.2021.30, 2022.

Agiadi, K., Vasiliev, I., Butiseacă, G., Kontakiotis, G., Thivaiou, D., Besiou, E., Zarkogiannis, S., Koskeridou, E., Antonarakou, A., Mulch, A.: Dataset for Agiadi et al._Coupled otolith and foraminifera oxygen and carbon stable isotopes evidence paleoceanographic changes and fish metabolic responses, Zenodo Repository, https://doi.org/10.5281/zenodo.10602427.

Antonarakou, A., Kontakiotis, G., Vasilatos, C., Besiou, E., Zarkogiannis, S., Drinia, H., Mortyn, P. G., Tsaparas, N., Makri, P., and Karakitsios, V.: Evaluating the Effect of Marine Diagenesis on Late Miocene Pre-Evaporitic Sedimentary Successions of Eastern Mediterranean Sea, IOP Conf. Ser. Earth Environ. Sci., 221, 012051, https://doi.org/10.1088/1755-1315/221/1/012051, 2019.

Bulian, F., Sierro, F. J., Ledesma, S., Jiménez-Espejo, F. J., and Bassetti, M.-A.: Messinian West Alboran Sea record in the proximity of Gibraltar: Early signs of Atlantic-Mediterranean gateway restriction, Mar. Geol., 434, 106430, https://doi.org/10.1016/j.margeo.2021.106430, 2021.

Bulian, F., Kouwenhoven, T. J., Jiménez-Espejo, F. J., Krijgsman, W., Andersen, N., and Sierro, F. J.: Impact of the Mediterranean-Atlantic connectivity and the late Miocene carbon shift on deep-sea communities in the Western Alboran Basin, Palaeogeogr. Palaeoclimatol. Palaeoecol., 589, 110841, https://doi.org/10.1016/j.palaeo.2022.110841, 2022.

Bulian, F., Jiménez-Espejo, F. J., Andersen, N., Larrasoaña, J. C., and Sierro, F. J.: Mediterranean water in the Atlantic Iberian margin reveals early isolation events during the Messinian Salinity Crisis, Glob. Planet. Change, 231, 104297, https://doi.org/10.1016/j.gloplacha.2023.104297, 2023.

Burton, T., Killen, S. S., Armstrong, J. D., and Metcalfe, N. B.: What causes intraspecific variation in resting metabolic rate and what are its ecological consequences?, Proc. R. Soc. B Biol. Sci., 278, 3465–3473, https://doi.org/10.1098/rspb.2011.1778, 2011.

Butiseacă, G. A., van der Meer, M. T. J., Kontakiotis, G., Agiadi, K., Thivaiou, D., Besiou, E., Antonarakou, A., Mulch, A., and Vasiliev, I.: Multiple Crises Preceded the Mediterranean Salinity Crisis: Aridification and Vegetation Changes Revealed by Biomarkers and Stable Isotopes, Glob. Planet. Change, 2022.

Campana, S. E.: Chemistry and composition of fish otoliths: pathways, mechanisms and applications, Mar. Ecol. Prog. Ser., 188, 263–297, 1999.

Chung, M.-T., Trueman, C. N., Godiksen, J. A., Holmstrup, M. E., and Grønkjær, P.: Field metabolic rates of teleost fishes are recorded in otolith carbonate, Commun. Biol., 2, 1–10, https://doi.org/10.1038/s42003-018-0266-5, 2019a.

Chung, M.-T., Trueman, C. N., Godiksen, J. A., Grønkjær, P., Chung, M.-T., Trueman, C. N., Godiksen, J. A., and Grønkjær, P.: Otolith δ13C values as a metabolic proxy: approaches and mechanical underpinnings, Mar. Freshw. Res., 70, 1747–1756, https://doi.org/10.1071/MF18317, 2019b.

Cornée, J.-J., Quillévéré, F., Moissette, P., Fietzke, J., López-Otálvaro, G. E., Melinte-Dobrinescu, M., Philippon, M., Hinsbergen, D. J. J. van, Agiadi, K., Koskeridou, E., and Münch, P.: Tectonic motion in oblique subduction forearcs: insights from the revisited Middle and Upper Pleistocene deposits of Rhodes, Greece, J. Geol. Soc., 176, 78–96, https://doi.org/10.1144/jgs2018-090, 2019.

Darnaude, A. M., Sturrock, A., Trueman, C. N., Mouillot, D., EIMF, Campana, S. E., and Hunter, E.: Listening in on the past: What can otolith δ18O values really tell us about the environmental history of fishes?, PLOS ONE, 9, e108539, https://doi.org/10.1371/journal.pone.0108539, 2014.

Drury, A. J., Westerhold, T., Hodell, D., and Röhl, U.: Reinforcing the North Atlantic backbone: revision and extension of the composite splice at ODP Site 982, Clim Past, 14, 321–338, https://doi.org/10.5194/cp-14-321-2018, 2018.

Edelist, D.: New length–weight relationships and Lmax values for fishes from the Southeastern Mediterranean Sea, J. Appl. Ichthyol., 30, 521–526, https://doi.org/10.1111/j.1439-0426.2012.02060.x, 2014.

Elderfield, H., Vautravers, M., and Cooper, M.: The relationship between shell size and Mg/Ca, Sr/Ca, δ18O, and δ13C of species of planktonic foraminifera, Geochem. Geophys. Geosystems, 3, 1–13, https://doi.org/10.1029/2001GC000194, 2002.

Flecker, R., Krijgsman, W., Capella, W., de Castro Martíns, C., Dmitrieva, E., Mayser, J. P., Marzocchi, A., Modestu, S., Ochoa, D., Simon, D., Tulbure, M., van den Berg, B., van der Schee, M., de Lange, G., Ellam, R., Govers, R., Gutjahr, M., Hilgen, F., Kouwenhoven, T., Lofi, J., Meijer, P., Sierro, F. J., Bachiri, N., Barhoun, N., Alami, A. C., Chacon, B., Flores, J. A., Gregory, J., Howard, J., Lunt, D., Ochoa, M., Pancost, R., Vincent, S., and Yousfi, M. Z.: Evolution of the Late Miocene

Mediterranean-Atlantic gateways and their impact on regional and global environmental change, Earth-Sci. Rev., 150, 365–392, https://doi.org/10.1016/j.earscirev.2015.08.007, 2015.

FishBase: www.fishbase.org, last access: 10 January 2024.

Gauldie, R. W.: Biological factors controlling the carbon isotope record in fish otoliths: Principles and evidence, Comp. Biochem. Physiol. B Biochem. Mol. Biol., 115, 201–208, https://doi.org/10.1016/0305-0491(96)00077-6, 1996.

Girone, A., Nolf, D., and Cavallo, O.: Fish otoliths from the pre-evaporitic (Early Messinian) sediments of northern Italy: Their stratigraphic and palaeobiogeographic significance, Facies, 56, 399–432, https://doi.org/10.1007/s10347-010-0212-6, 2010.

Herbert, T. D., Lawrence, K. T., Tzanova, A., Peterson, L. C., Caballero-Gill, R., and Kelly, C. S.: Late Miocene global cooling and the rise of modern ecosystems, Nat. Geosci., 9, ngeo2813, https://doi.org/10.1038/ngeo2813, 2016.

Hodell, D., Curtis, J., Sierro, F., and Raymo, M.: Correlation of late Miocene to early Pliocene sequences between the Mediterranean and North Atlantic, Paleoceanography, 16, 164–178, https://doi.org/10.1029/1999PA000487, 2001.

Hsü, K. J., Ryan, W. B. F., and Cita, M. B.: Late Miocene Desiccation of the Mediterranean, Nature, 242, 240–244, https://doi.org/10.1038/242240a0, 1973.

Ilyina, L. B., Shcherba, I. G., and Khondkarian, S. O.: Map 8: Middle late Miocene (late Tortonian - early Messinian - early Maeotian - late Pannonian) in Lithological-Paleogeographic maps of Paratethys. In: Popov, S.V., Rögl, F., Rozanov, A.Y., Steininger, F.F., Shcherba, I.G., Kovac, M. (Eds.), Cour. Forschungsinstitut Senckenberg, 250, 2004.

Jones, J., Hunter, E., Hambach, B., Wilding, M., and Trueman, C. N.: Individual variation in field metabolic rates of wild living fish have phenotypic and ontogenetic underpinnings: insights from stable isotope compositions of otoliths, Front. Ecol. Evol., 11, 2023.

Kalish, J. M.: Oxygen and carbon stable isotopes in the otoliths of wild and laboratory-reared Australian salmon (Arripis trutta), Mar. Biol., 110, 37–47, https://doi.org/10.1007/BF01313090, 1991.

Karakitsios, V., Roveri, M., Lugli, S., Manzi, V., Gennari, R., Antonarakou, A., Triantaphyllou, M., Agiadi, K., Kontakiotis, G., Kafousia, N., and de Rafelis, M.: A record of the Messinian salinity crisis in the eastern Ionian tectonically active domain (Greece, eastern Mediterranean), Basin Res., 29, 203–233, https://doi.org/10.1111/bre.12173, 2017.

AquaMaps: predicted range maps for aquatic species: www.aquamaps.org.

Kerr, R. A.: Unmasking a Shifty Climate System, Science, 255, 1508–1510, https://doi.org/10.1126/science.255.5051.1508, 1992.

Kontakiotis, G., Butiseacă, G. A., Antonarakou, A., Agiadi, K., Zarkogiannis, S. D., Krsnik, E., Besiou, E., Zachariasse, W. J., Lourens, L., Thivaiou, D., Koskeridou, E., Moissette, P., Mulch, A., Karakitsios, V., and Vasiliev, I.: Hypersalinity accompanies tectonic restriction in the eastern Mediterranean prior to the Messinian Salinity Crisis, Palaeogeogr. Palaeoclimatol. Palaeoecol., 592, 110903, https://doi.org/10.1016/j.palaeo.2022.110903, 2022.

Kouwenhoven, T. J., Hilgen, F. J., and van der Zwaan, G. J.: Late Tortonian–early Messinian stepwise disruption of the Mediterranean–Atlantic connections: constraints from benthic foraminiferal and geochemical data, Palaeogeogr. Palaeoclimatol. Palaeoecol., 198, 303–319, https://doi.org/10.1016/S0031-0182(03)00472-3, 2003.

Krijgsman, W., Hilgen, F. J., Raffi, I., Sierro, F. J., and Wilson, D. S.: Chronology, causes and progression of the Messinian salinity crisis, Nature, 400, 652–655, https://doi.org/10.1038/23231, 1999.

Kroopnick, P. M.: The distribution of 13C of ΣCO2 in the world oceans, Deep Sea Res. Part Oceanogr. Res. Pap., 32, 57–84, https://doi.org/10.1016/0198-0149(85)90017-2, 1985.

Landini, W. and Sorbini, C.: Evolutionary dynamics in the fish faunas of the Mediterranean basin during the Plio-Pleistocene, Quat. Int., 140–141, 64–89, https://doi.org/10.1016/j.quaint.2005.05.019, 2005.

Lanzante, J. R.: Resistant, Robust and Non-Parametric Techniques for the Analysis of Climate Data: Theory and Examples, Including Applications to Historical Radiosonde Station Data, Int. J. Climatol., 16, 1197–1226, https://doi.org/10.1002/(SICI)1097-0088(199611)16:11<1197::AID-JOC89>3.0.CO;2-L, 1996.

Laskar, J., Robutel, P., Joutel, F., Gastineau, M., Correia, A. C. M., and Levrard, B.: A long-term numerical solution for the insolation quantities of the Earth, Astron. Astrophys., 428, 261–285, https://doi.org/10.1051/0004-6361:20041335, 2004.

Lyu, J., Kouwenhoven, T. J., Calieri, R., and Lourens, L. J.: Foraminifera of the Faneromeni section (Crete, Greece) reflect the palaeoenvironmental development towards the Messinian salinity crisis, Mar. Micropaleontol., 172, 102107, https://doi.org/10.1016/j.marmicro.2022.102107, 2022.

Mackensen, A. and Schmiedl, G.: Stable carbon isotopes in paleoceanography: atmosphere, oceans, and sediments, Earth-Sci. Rev., 197, 102893, https://doi.org/10.1016/j.earscirev.2019.102893, 2019.

Mancini, A. M., Gennari, R., Lozar, F., Natalicchio, M., Della Porta, G., Bernasconi, D., Pellegrino, L., Dela Pierre, F., Martire, L., and Negri, A.: Sensitivity of the thermohaline circulation during the Messinian: Toward constraining the dynamics of Mediterranean deoxygenation, Deep Sea Res. Part Oceanogr. Res. Pap., 203, 104217, https://doi.org/10.1016/j.dsr.2023.104217, 2024.

Martino, J. C., Doubleday, Z. A., and Gillanders, B. M.: Metabolic effects on carbon isotope biomarkers in fish, Ecol. Indic., 97, 10–16, https://doi.org/10.1016/j.ecolind.2018.10.010, 2019.

Martino, J. C., Doubleday, Z. A., Chung, M.-T., and Gillanders, B. M.: Experimental support towards a metabolic proxy in fish using otolith carbon isotopes, J. Exp. Biol., 223, jeb217091, https://doi.org/10.1242/jeb.217091, 2020.

Mirasole, A., Gillanders, B. M., Reis-Santos, P., Grassa, F., Capasso, G., Scopelliti, G., Mazzola, A., and Vizzini, S.: The influence of high pCO2 on otolith sha pe, chemical and carbon isoto pe com position of six coastal fish s pecies in a Mediterranean shallow CO2 vent, Mar. Biol., 164, 191, https://doi.org/10.1007/s00227-017-3221-y, 2017.

Moissette, P., Cornée, J.-J., Antonarakou, A., Kontakiotis, G., Drinia, H., Koskeridou, E., Tsourou, T., Agiadi, K., and Karakitsios, V.: Palaeoenvironmental changes at the Tortonian/Messinian boundary: A deep-sea sedimentary record of the eastern Mediterranean Sea, Palaeogeogr. Palaeoclimatol. Palaeoecol., 505, 217–233, https://doi.org/10.1016/j.palaeo.2018.05.046, 2018.

R Development Core Team: R: A language and environment for statistical computing, 2023.

Radtke, R. L., Lenz, P., Showers, W., and Moksness, E.: Environmental information stored in otoliths: insights from stable isotopes, Mar. Biol., 127, 161–170, https://doi.org/10.1007/BF00993656, 1996.

Rodionov, S. N.: A sequential algorithm for testing climate regime shifts, Geophys. Res. Lett., 31, https://doi.org/10.1029/2004GL019448, 2004.

Room, A., Franco-Gaviria, F., and Urrego, D.: rshift: paleoecology and regime shift analysis, 2020.

Sabino, M., Dela Pierre, F., Natalicchio, M., Birgel, D., Gier, S., and Peckmann, J.: The response of water column and sedimentary environments to the advent of the Messinian salinity crisis: insights from an onshore deep-water section (Govone, NW Italy), Geol. Mag., 1–17, https://doi.org/10.1017/s0016756820000874, 2020.

van der Schee, M., Sierro, F. J., Jiménez-Espejo, F. J., Hernández-Molina, F. J., Flecker, R., Flores, J. A., Acton, G., Gutjahr, M., Grunert, P., García-Gallardo, Á., and Andersen, N.: Evidence of early bottom water current flow after the Messinian Salinity Crisis in the Gulf of Cadiz, Mar. Geol., 380, 315–329, https://doi.org/10.1016/j.margeo.2016.04.005, 2016.

Scheffer, M.: Critical Transitions in Nature and Society, Princeton University Press, 398 pp., 2020.

Schouten, S., Hopmans, E. C., Schefuß, E., and Sinninghe Damsté, J. S.: Distributional variations in marine crenarchaeotal membrane lipids: a new tool for reconstructing ancient sea water temperatures?, Earth Planet. Sci. Lett., 204, 265–274, https://doi.org/10.1016/S0012-821X(02)00979-2, 2002.

Schwarzhans, W., Agiadi, K., and Carnevale, G.: Late Miocene–Early Pliocene evolution of Mediterranean gobies and their environmental and biogeographic significance, Riv. Ital. Paleontol. E Stratigr., 126, https://doi.org/10.13130/2039-4942/14185, 2020.

Seidenkrantz, M.-S., Kouwenhoven, T. J., Jorissen, F. J., Shackleton, N. J., and van der Zwaan, G. J.: Benthic foraminifera as indicators of changing Mediterranean–Atlantic water exchange in the late Miocene, Mar. Geol., 163, 387–407, https://doi.org/10.1016/S0025-3227(99)00116-4, 2000.

Sierro, F. J., Flores, J. A., Francés, G., Vazquez, A., Utrilla, R., Zamarreño, I., Erlenkeuser, H., and Barcena, M. A.: Orbitally-controlled oscillations in planktic communities and cyclic changes in western Mediterranean hydrography during the Messinian, Palaeogeogr. Palaeoclimatol. Palaeoecol., 190, 289–316, https://doi.org/10.1016/S0031-0182(02)00611-9, 2003.

Smoliński, S., Denechaud, C., Leesen, G. von, Geffen, A. J., Grønkjær, P., Godiksen, J. A., and Campana, S. E.: Differences in metabolic rate between two Atlantic cod (Gadus morhua) populations estimated with carbon isotopic composition in otoliths, PLOS ONE, 16, e0248711, https://doi.org/10.1371/journal.pone.0248711, 2021.

Solomon, C. T., Weber, P. K., Joseph J Cech, J., Ingram, B. L., Conrad, M. E., Machavaram, M. V., Pogodina, A. R., and Franklin, R. L.: Experimental determination of the sources of otolith carbon and associated isotopic fractionation, Can. J. Fish. Aquat. Sci., 63, 79–89, https://doi.org/10.1139/f05-200, 2006.

Thorrold, S. R. a, Campana, S. E. b, Jones, C. M. a, and Swart, P. K. c: Factors determining δ 13C and δ 18O fractionation in aragonitic otoliths of marine fish, Geochim. Cosmochim. Acta, 61, 2909–2919, 1997.

Trueman, C. N., Chung, M.-T., and Shores, D.: Ecogeochemistry potential in deep time biodiversity illustrated using a modern deep-water case study, Philos. Trans. R. Soc. B Biol. Sci., 371, 20150223, https://doi.org/10.1098/rstb.2015.0223, 2016.

Trueman, C. N., Artetxe-Arrate, I., Kerr, L. A., Meijers, A. J. S., Rooker, J. R., Sivankutty, R., Arrizabalaga, H., Belmonte, A., Deguara, S., Goñi, N., Rodriguez-Marin, E., Dettman, D. L., Santos, M. N., Karakulak, F. S., Tinti, F., Tsukahara, Y., and Fraile, I.: Thermal sensitivity of field metabolic rate predicts differential futures for bluefin tuna juveniles across the Atlantic Ocean, Nat. Commun., 14, 7379, https://doi.org/10.1038/s41467-023-41930-2, 2023.

Vasiliev, I., Karakitsios, V., Bouloubassi, I., Agiadi, K., Kontakiotis, G., Antonarakou, A., Triantaphyllou, M., Gogou, A., Kafousia, N., Rafélis, M. de, Zarkogiannis, S., Kaczmar, F., Parinos, C., and Pasadakis, N.: Large Sea Surface Temperature, Salinity, and Productivity-Preservation Changes Preceding the Onset of the Messinian Salinity Crisis in the Eastern Mediterranean Sea, Paleoceanogr. Paleoclimatology, 34, 182–202, https://doi.org/10.1029/2018PA003438, 2019.

Wickham, H., Francois, R., Henry, L., Muller, K., and Vaughan, D.: dplyr: A Grammar of Data Manipulation, 2023.

Wurster, C. M. and Patterson, W. P.: Metabolic rate of late Holocene freshwater fish: evidence from δ13C values of otoliths, Paleobiology, 29, 492–505, https://doi.org/10.1666/0094-8373(2003)029<0492:MROLHF>2.0.CO;2, 2003.

Zachariasse, W. J., Kontakiotis, G., Lourens, L. J., and Antonarakou, A.: The Messinian of Agios Myron (Crete, Greece): A key to better understanding of diatomite formation on Gavdos (south of Crete), Palaeogeogr. Palaeoclimatol. Palaeoecol., 581, 110633, https://doi.org/10.1016/j.palaeo.2021.110633, 2021.